Journal of Photopolymer Science and Technology
Volume 31, Number 6 (2018) 669 – 678 ©2018SPST

Ferrocene Bearing Non-ionic Poly-aryl Tosylates: Synthesis, Characterization and Electron Beam Lithography Applications

Pulikanti Guruprasad Reddy[1], M. G. Moinuddin[2], Aneesh M. Joseph[3], Santu Nandi[1], Subrata Ghosh[1], Chullikkattil P. Pradeep[1*], Satinder K. Sharma[2], and Kenneth E. Gonsalves[1***]**

[1]School of Basic Sciences,
[2]School of Computing and Electrical Engineering,
Indian Institute of Technology Mandi, Mandi-175005, Himachal Pradesh, India
**pradeep@iitmandi.ac.in, ***kenneth@iitmandi.ac.in*
[3]Centre of Excellence in Nanoelectronics, Department of Electrical Engineering,
Indian Institute of Technology Bombay, Powai-400076, Maharashtra, India
***satinder@iitmandi.ac.in*

The development of new organic-inorganic hybrid photoresists with optimal lithographic performances is an extremely important but challenging task. In this regard, we have synthesized a new family of homo- and hybrid-polymer resists based on 4-(tosyloxy)phenyl methacrylate (TPMA) and ferrocene methacrylate (FEMA) monomers for micro-/nano-lithography applications. The homo polymer resist, poly(TPMA), was synthesized by a free radical polymerization of TPMA monomer in ACN/THF (2:1, v/v) solvent system using azobisisobutyronitrile (AIBN) as the radical initiator. The hybrid copolymer resists, 2.0%-&4.0%-poly(FEMA-*co*-TPMA), containing 2.0 and 4.0 weight percentages of FEMA respectively, were synthesized by reacting FEMA (10 and 20% initial feed ratios respectively) and TPMA (90 and 80% initial feed ratios respectively) under similar reaction conditions. The ferrocene contents of the hybrid copolymers were calculated by proton NMR analysis. The potential of these polymer resists to pattern micro- and nano-features were tested under deep ultraviolet (DUV) and electron beam (e-beam) lithography tools respectively. The thin films formed by 4.0%-poly(FEMA-*co*-TPMA) exhibited high surface roughness in comparison to those of poly(TPMA) and 2.0%-poly(FEMA-*co*-TPMA) resists, probably due to the high ferrocene content of the former. The scanning electron microscopy (SEM) analysis of the e-beam exposed (dose 950 $\mu C/cm^2$) thin films of poly(TPMA) revealed patterning of 40 nm (L/10S to L/4S), 30 nm (L/10S & L/5S) and 22 nm (L/10S) line features. Similarly, 2.0%-poly(FEMA-*co*-TPMA) patterned 40 nm (L/5S to L/S), 30 (L/5S to L/S) and 20 nm (L/5S & L/4S) line features under the e-beam exposure (dose 500 $\mu C/cm^2$). The sensitivity and contrast values were calculated from the normalized remaining thickness (NRT) curve analysis as 270 $\mu C/cm^2$; 5.2 and 153 $\mu C/cm^2$; 1.98 respectively for poly(TPMA) and 2.0%-poly(FEMA-*co*-TPMA) resists. The present study therefore reveals that the incorporation of small amounts of ferrocene into the poly-aryl tosylate based resist formulations helps to enhance its sensitivity and resolution.

Keywords: Organic-inorganic hybrid resists, Non-ionic poly-aryl tosylates, Deep ultraviolet lithography, Electron beam lithography, Ferrocene

1. Introduction

Semiconductor industry has progressed remarkably over the past few decades in terms of the development of efficient integrated circuits (ICs) with reduced dimensions for various consumer electronics applications [1,2].

Received May 2, 2018
Accepted June 25, 2018

Photolithography is a key technology in the development of ICs, which in turn depends on the advancements in lithographic patterning tools as well as photoresist technology [3-6]. The international technology roadmap for semiconductors-2015 (ITRS-2015) predicts the achievement of sub-7 nm patterning resolution in near future [7,8]. The development of novel photoresist materials to achieve this ambitious target is therefore an important research area. Till date, a number of organic photoresists, either chemically amplified resists (CARs) [9-12] or non-chemically amplified resists (n-CARs) [5,6], have been reported for lithographic applications. However, due to poor resolution, sensitivity and etch resistance characteristics, the applicability of many of such resist materials are limited for patterning sub-20 nm features [13-20].

Incorporation of inorganic components into the organic resist formulations is a well-accepted strategy towards the development of improved photo-resist materials [6,21-23]. High optical densities of the metal ions help the resist materials to harvest photons more efficiently and enhance their sensitivities [6,24-26]. Various inorganic moieties including metaloxide nanoparticles, metal clusters, organometallic species etc. have been successfully tested in resist formulations for improving their lithographic performances [24-28]. In addition to the polymer based hybrid resists, hybrid molecular resists have also been tested for high resolution lithographic applications. For example, Brainard *et al.* have reported a series of hybrid molecular resists based on Pt, Pd, Co, Sn, and Sb for high-resolution extreme ultraviolet lithography (EUVL) applications [26,29-31]. Similarly, HfO_2, ZrO_2, TiO_2, ZnO_2 etc. nano particles based hybrids have also been tested for sub-20 nm patterning applications successfully [6,32,33]. Therefore, the development of new hybrid photoresists using newer inorganic entities is indeed a promising approach for achieving the targets set by ITRS-2015.

Polymers incorporating organometallic compounds (OMCs) have received great attention in recent years because of their applications in diverse areas including materials science, catalysis, and semiconductor supported devices [34,35]. Ferrocene is an attractive and versatile OMC owing to its stable redox properties, good solubility and susceptibility for chemical modifications [36-38]. Ferrocene having a central metal ion (Fe^{2+}) has a high optical density (6-8) compared to that of carbon (0-2) and hence it may act as sensitivity enhancer in photoresist formulations. However, reports on ferrocenyl derivatives as sensitivity enhancers in photoresist formulations are scarce in the literature [39-42]. J. Zhang *et al.* have developed a metal carbonyl polymer, PFpP, having high plasma etch resistance for high-resolution e-beam lithography applications [39]. Recently, our group had reported a hybrid copolymer resist, poly(MAPDST-*co*-FMMA), bearing a ferrocene monomer (FMMA), which offered high thermal stability and sensitivity as compared to the parent resist, poly(MAPDST) [40].

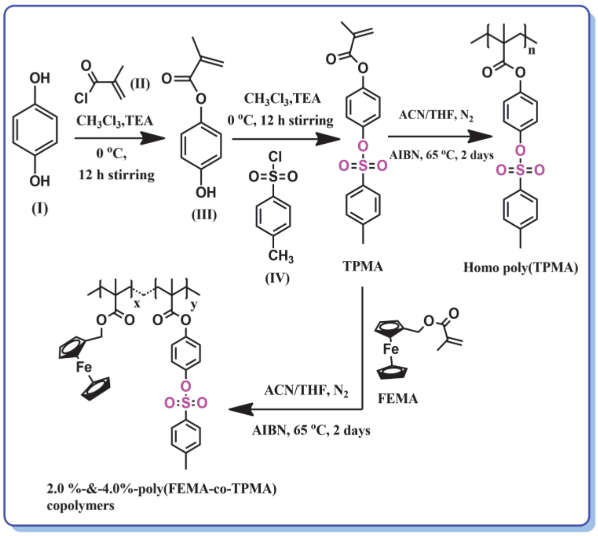

Scheme 1. Chemical synthetic route for poly-(TPMA) and 2.0%-&-4.0%-poly-(FEMA-*co*-TPMA) copolymer resists.

Meanwhile, imino/imido sulfonates and tosylates are gaining interest in photoresist technology [43,44]. Due to properties like high thermal stability and solubility, they are used as alternative photoacid generators (PAGs) in place of sulfonium/iodonium triflate based PAGs. However, the concept of non-ionic PAG based polymer resists has not been explored in detail yet. Considering the above, the present work focuses on the synthesis of non-ionic aryl tosylate (4-(tosyloxy)phenyl methacrylate (TPMA)) and ferrocene methacrylate (FEMA) based homo and hybrid copolymer resists, i.e. poly(TPMA) and 2.0%-&4.0%-poly(FEMA-*co*-TPMA), for micro/nanolithography applications. These polymers are expected to act as good photoresists as the aromatic sulfonates can undergo structural decomposition upon interaction with high-energy radiations leading to polarity change. It is also expected that the incorporation of inorganic FEMA units in poly(TPMA) may lead to improved lithography properties as compared to the neat homo poly(TPMA) resist. The details of these studies and the results are presented in the following sections.

2. Experimental

2.1. Chemicals and reagents

Hydroquinone (**I**), *p*-toluenesulfonyl chloride (**IV**) and triethyl amine were purchased from Sigma Aldrich, India. Methacryloyl chloride (**II**) was purchased from Avra Synthesis Pvt Ltd, India. HPLC grade acetonitrile, chloroform, tertahydrofuran, and 1,4-dioxane were purchased from Merck, India and used as received. 4-Hydroxyphenyl methacrylate (**III**), 4-(tosyloxy)phenyl methacrylate (TPMA), and ferrocene methacrylate (FEMA) were synthesized according to the published protocols [40,45]. AIBN (azobisisobutryronitrile) was purchased from Paras Polymers, India and recrystallized twice before use in polymerizations.

2.2. Instrumentation details

Fourier transform infrared (FT-IR) spectra were recorded on a Perkin-Elmer Spectrum-2 spectrophotometer. $^{1}H/^{13}C$ NMR analyses were performed on JEOL JNM ECX 500 MHz nuclear magnetic resonance (NMR) spectrometer in DMSO-d_6/$CDCl_3$ solvents. Molecular weights (Mw) and polydispersity indices (PDI) of the polymers were determined by using gel permeation chromatography (GPC) with Agilent 1260 Infinity Series instrument. PL gel mixed B column with a pore size 10 μm was used for the molecular weight determinations. 0.1% Lithium bromide (LiBr) in dimethyl formamide (DMF) was used as the mobile phase at a flow rate of 1 mL/min at a column temperature of 70 ºC. Thermogravimetric analyses (TGA) and differential scanning calorimetry (DSC) experiments were performed on Netzsch Model STA 449 F1 JUPITER Series instrument. The heating rate employed was 10 °C/min under N_2 atmosphere over a temperature range of 25 to 800 °C. Photoresist film thickness measurements were performed by using NanoMap-D stylus profilometer. RAITH150 two e-beam patterning tool was used for nanolithography investigations within the dose range 100-1000 $\mu C/cm^2$. QUANTA 200FEG FE-SEM instrument and Bruker Dimension Icon Atomic Force Microscope (AFM) tools were used for imaging the critical dimensions patterned on the silicon substrate. Energy dispersive X-ray (EDX) spectroscopy analyses of the hybrid copolymer resists were conducted on FEI-Nova nano SEM-450.

2.3. Synthesis of poly(TPMA)

Poly(TPMA) was synthesized by following a published protocol [45] with some modifications. The typical synthetic procedure employed was as follows: 1 g of TPMA and AIBN (2 wt% relative to the monomer weight) were taken in a round bottom flask under N_2 atmosphere in darkness. To this, 15 mL dry THF/ACN (1:2, v/v) solvent mixture was added and stirred to get a clear solution. Thereafter, the reaction mixture was filtered through 0.4 μm Teflon filter and transferred to a polymerization vessel with a side arm neck. After several rounds of freeze-thaw cycles (6-7 cycles) with N_2 purging, the reaction mixture was allowed to stir for 2 days at 65 ºC. Finally, the reaction mixture was poured into 200 mL of petroleum ether and the resultant white solid was washed several times with petroleum ether and dried at 50 ºC overnight in a temperature controlled hot air oven. Yield: 73%. FT-IR: ν max/cm^{-1} 2949 (ν $-CH_3$), 1747 (ν C=O), 1597-1494-1451 (ν C=C), 1293 (ν C–O), 1159 (ν S=O), 1088, 1014, 966, 866, 809, 728, 694, 658, 548 cm^{-1}. ^{1}H NMR (500 MHz, $CDCl_3$) δ_H = 7.71 (s, 2H, ArH), 7.31 (s, 2H, ArH), 6.94 (s, 4H, ArH) 2.43 (s, 3H, Ar–CH_3), 2.2-1.7 (m, 2H, $-CH_2-$ polymeric), 1.4-1.19 (m, 3H, $-CH_3$ polymeric); ^{13}C NMR (125 MHz, $CDCl_3$) δ_C = 175.17 (C=O), 148.84, 147.02, 145.88, 132.19, 130.07, 128.49, 123.65, 122.46, 65.94, 45.77, 21.81, 20.41, 18.81, 15.3.

2.4. Synthesis of 2.0%-poly(FEMA-*co*-TPMA)

The hybrid copolymer 2.0%-poly(FEMA-*co*-TPMA) was also synthesized by following the general polymerization procedure employed for poly(TPMA), by reacting the organic monomer TPMA (90%, 2.71 mmol) with the hybrid OMC monomer FEMA (10%, 0.35 mmol) in presence of AIBN (2 wt%, relative to both the monomers) as the free radical initiator at 65 ºC under N_2 atmosphere for 2 days. Brown colored solid. Yield: 54%. FT-IR: ν max/cm^{-1} 2952 (ν $-CH_3$), 1748 (ν C=O), 1597-1495-1450 (ν C=C), 1371-1293 (*v* C-O), 1160 (*v* S=O), 1089, 1014 (substituted and unsubstituted cp ring with Fe), 964, 867, 810, 728, 694, 658, 581, 550, 514 cm^{-1}. ^{1}H NMR (500 MHz, DMSO-d_6) δ_H = 7.7 (br s, 2H, ArH), 7.4 (br s, 2H, ArH), 7.1-6.6 (m, 4H, ArH), 4.20 (s, 2H, ferrocene CH_2), 4.1 (s, 9H, ferrocene), 2.3 (s, 3H, Ar–CH_3), 1.5-1.0 (m, 5H, –CH_2– and –CH_3 polymeric); ^{13}C NMR (125 MHz, DMSO-d_6) δ_C = 174.91, 174.20 (C=O), 156.17, 148.51, 145.88, 141.17, 131.26, 130.20, 128.24, 123.04, 122.59, 115.93, 68.19, 64.92, 45.08, 21.10, 19.32, 18.06, 15.16.

2.5. Synthesis of 4.0%-poly(FEMA-*co*-TPMA)

The hybrid copolymer 4.0%-poly(FEMA-*co*-TPMA) was synthesized by following the general polymerization procedure employed for 2.0%-poly(FEMA-*co*-TPMA), by reacting the organic monomer TPMA (80%, 2.40 mmol) with the hybrid ferrocene monomer FEMA (20%, 0.70 mmol) in presence of AIBN (2 wt%, relative to both the monomers) as the free radical initiator at 65 °C under N_2 atmosphere for 2 days. Brown colored solid. Yield: 61%. FT-IR: *v* max/cm^{-1} 2932 (*v* –CH_3), 1749 (*v* C=O), 1597-1495-1450 (*v* C=C), 1371-1293 (*v* C-O), 1160 (*v* S=O), 1089, 1014 (substituted and unsubstituted cp ring with Fe), 964, 867, 842, 810, 729, 694, 658, 580, 550, 514 cm^{-1}. ^{1}H NMR (500 MHz, DMSO-d_6) δ_H = 7.6 (br s, 2H, ArH), 7.4 (br s, 2H, ArH), 7.0-6.6 (br m, 4H, ArH), 4.2 (br s, 2H, ferrocene O–CH_2), 4.1-4.0 (br m, 9H, ferrocene protons), 2.4-2.3 (br peak, 3H, Ar–CH_3), 1.3-1.0 (br m, 2H, –CH_2– polymeric), 0.82 (s, 3H, –CH_3 polymeric); ^{13}C NMR (125 MHz, DMSO-d_6) δ_C = 174.5, 173.5 (C=O), 146.40, 145.86, 141.19, 131.29, 130.22, 130.13, 128.26, 127.96, 123.38, 123.06, 122.48, 115.94, 45.22, 30.98, 21.17, 13.99.

3. Results and discussion

3.1. Synthesis and characterization

The homo polymer poly(TPMA) and the hybrid copolymers 2.0%-&4.0%-poly(FEMA-*co*-TPMA) were synthesized by AIBN initiated free radical polymerization starting from the monomers TPMA (for homo polymer) and TPMA & FEMA (for hybrid polymers) in dry ACN/THF (2:1, v/v) at 65 °C under inert atmosphere (Scheme 1). The feed ratio of the inorganic ferrocene monomer used for the synthesis of 2.0%-&4.0%-poly(FEMA-*co*-TPMA) copolymers were 10% and 20%, respectively. The synthesized polymers were thoroughly characterized by using various analytical and spectroscopic techniques including IR, TGA, DSC, NMR, GPC, and EDX analyses.

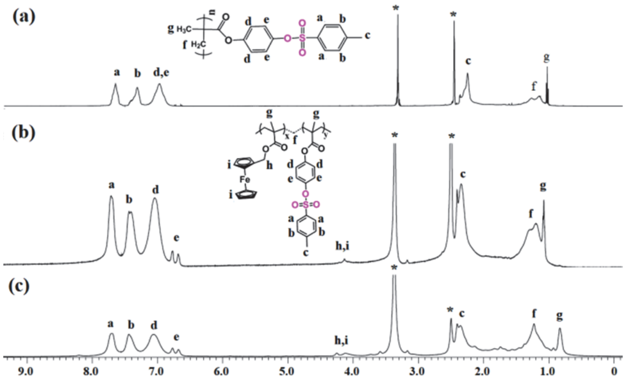

Fig. 1. ^{1}H NMR spectra of (a) poly(TPMA), (b) 2.0%-poly(FEMA-*co*-TPMA), and (c) 4.0%-poly(FEMA-*co*-TPMA).

The functional groups present in poly(TPMA) and 2.0%-&4.0%-poly(FEMA-*co*-TPMA) copolymers were characterized by FT-IR spectroscopy. The broad bands observed at 2949, 2952, and 2932 cm^{-1} correspond to the C–H vibrations. The vibrational bands observed in the range 1747-1750 cm^{-1} correspond to the carbonyl (C=O) functionality of the polymers. The aromatic C=C vibrations of the phenyl units appeared in the range 1450-1597 cm^{-1} for these polymers. The bands observed at 1290 cm^{-1} and 1159 cm^{-1} are due to C–O and S=O bonds respectively. The IR peak observed at 1014 cm^{-1} in the case of 2.0%-&4.0%-poly(FEMA-*co*-TPMA) hybrid copolymers is due to C–H vibrations of the cyclopentadienyl units of ferrocene [40].

The broad NMR signals observed for poly(TPMA) and 2.0%-&4.0%-poly(FEMA-*co*-TPMA) in the range 7.0-7.7 ppm correspond to the aromatic phenyl protons. The absence of any olefinic protons in the proton NMR of the polymers indicates the complete conversion of the monomers into polymer. The methyl protons of the aromatic tosylates appeared in the range 2.1-2.5 ppm. Similarly, the –CH_2– and –CH_3 protons of these polymers were observed in the range 2.0-1.5 ppm. In the case of hybrid copolymers, the proton signals observed at 5.00 ppm and 4.0-4.2 ppm correspond to O–CH_2 and cyclopentadienyl protons respectively, indicating the formation of these copolymers as expected (Fig. 1). The proton NMR analyses were also used to calculate the actual ferrocene contents in 2.0%-poly(FEMA-*co*-TPMA) and 4.0%-poly(FEMA-*co*-TPMA) (Table 1).

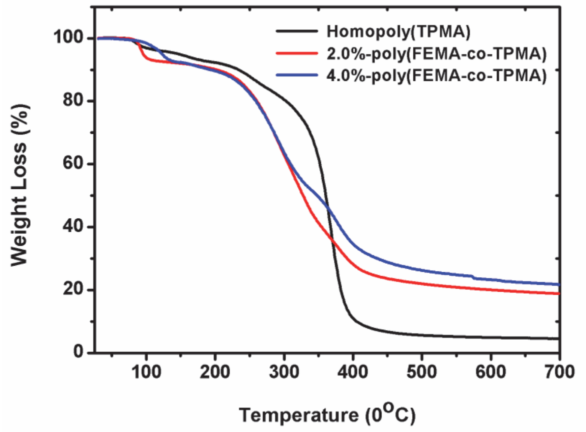

Fig. 2. TGA profiles of poly(TPMA) and 2.0%-&4.0%-poly(FEMA-*co*-TPMA) copolymers.

Weight average molecular weight (*M*w) of poly(TPMA) and 2.0%-&4.0%-poly(FEMA-*co*-TPMA) were calculated by using GPC analyses. Poly(ethyleneglycol) (PEG) and polyethylene oxide (PEO) were used as standards for plotting the size exclusion chromatography (SEC) calibration curve. The *M*w and polydispersity index (PDI) values of poly(TPMA), 2.0%-poly(FEMA-*co*-TPMA) and 4.0%-poly(FEMA-*co*-TPMA) were calculated as 14,759 g/mol, 1.73; 13,321 g/mol, 1.73; and 14,645 g/mol, 1.69 respectively (Table 1). The thermal stabilities of these polymers were determined by using TGA analyses. Experimental findings revealed that a major weight loss occurs for all these polymers in the temperature range 100-450 ºC. The residual mass observed beyond 400 ºC for 2.0%-poly(FEMA-*co*-TPMA) and 4.0%-poly(FEMA-*co*-TPMA) were higher compared to that observed of poly(TPMA), probably due to the ferrocene content of the formers as shown in Fig. 2.

Further, in order to confirm the presence and content of Fe element, we subjected the hybrid copolymers 2.0%-poly(FEMA-*co*-TPMA) and 4.0%-poly(FEMA-*co*-TPMA) for EDX analyses. The EDX profiles of 2.0%-poly(FEMA-*co*-TPMA) revealed the presence of C, O, S, and Fe elements with different weight compositions of 65.7%, 26.8%, 6.6%, and 0.8%, respectively (Fig. 3(a)). Similarly, the elemental composition of the hybrid copolymer 4.0%-poly(FEMA-*co*-TPMA) was analyzed as follows: C (66.2%), O (25.4%), S (6.5%), and Fe (1.7%) (Fig. 3 (b)). The EDX results therefore clearly conclude the incorporation of FEMA in the hybrid copolymer structures.

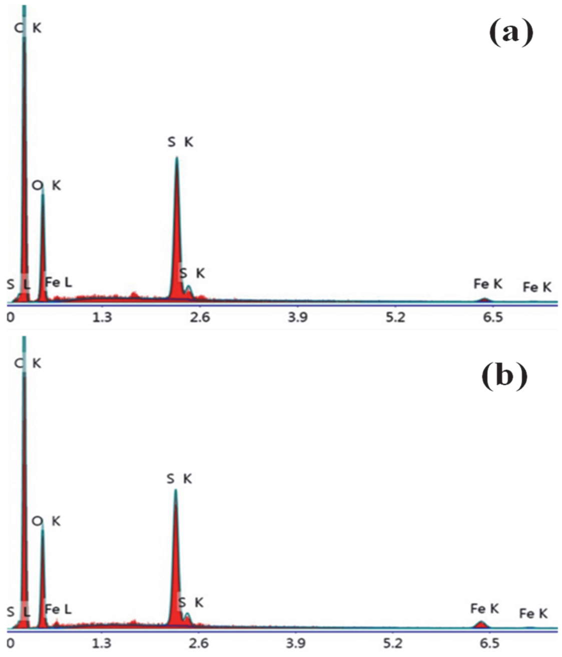

Fig. 3. EDX profiles of hybrid copolymers showing C, O, S, and Fe elements: (a) 2.0%-poly(FEMA-*co*-TPMA) copolymer; (b) 4.0%-poly(FEMA-*co*-TPMA) copolymer.

3.2. Lithography studies

After the successful synthesis and characterization, we tested the newly developed polymers as new n-CARs for micro- and nano-lithography applications. Resist formulations were prepared by dissolving the solid polymers in 1,4-dioxane (2 wt%) and these formulations were filtered twice by using 0.2 µm Teflon filters in order to remove any un-dissolved particles. The thin resist films of poly(TPMA) and 2.0%-&4.0%-poly(FEMA-*co*-TPMA) copolymers with thicknesses ~25 nm were achieved by spin coating the resist solutions onto silicon substrate at 5000 rpm for 60 sec. A pre-bake temperature of 80 °C was applied for 60

Table 1. Polymerization results of homo poly(TPMA) and hybrid 2.0%-&4.0%-poly(FEMA-*co*-TPMA) copolymer resists.

Name of the Polymer	Feed Ratio (wt%)		Copolymer Composition [a] (wt%)		Yield (%)	*M*w[b] (g/mol)/PDI[c]
	TPMA	FEMA	TPMA	FEMA		
Poly(TPMA)	100	-	100	-	73	14,759/1.73
2.0%-poly(FEMA-*co*-TPMA)	90	10	97.9	2.0	54	13,321/1.73
4.0%-poly(FEMA-*co*-TPMA)	80	20	96	4.0	61	14,645/1.68

[a] Polymer compositions were calculated by proton NMR analysis. [b] Weight average molecular weight (*M*w). [c] Polydispersity Index (PDI) were determined by GPC using DMF (0.1% LiBr) as a eluent and PEO & PEG as standards.

60 sec. to remove any excess of 1,4-dioxane present on the silicon substrate. Further, the quality of the resist thinfilms was analysed with AFM tool. AFM analyses revealed that the thinfilms formed by poly(TPMA) and 2.0%-poly(FEMA-*co*-TPMA) polymers are extremely smooth as compared to that formed by 4.0%-poly(FEMA-*co*-TPMA) polymer. The calculated film roughness of poly(TPMA), 2.0%-poly(FEMA-*co*-TPMA) and 4.0%-poly(FEMA-*co*-TPMA) polymers were 0.39, 0.42, and 1.80, respectively (not shown here). Perhaps due to the high ferrocene content, the 4.0%-poly(FEMA-*co*-TPMA) hybrid polymer formed a poor resist thin film with high roughness. Therefore, we excluded 4.0%-poly(FEMA-*co*-TPMA) hybrid copolymer from further lithographic analyses.

The initial lithographic evaluations of poly(TPMA) and 2.0%-poly(FEMA-*co*-TPMA) polymers as photoresists were conducted under deep ultraviolet (DUV-254 nm) lithography tool for micro-patterning applications. The resist samples were exposed to 254 nm light and the exposed samples were post-baked at 80 °C for 60 sec. Thereafter, the resist films were developed with 1,4-dioxane. We used 1,4-dioxane as the developer due to the poor developing behaviours of these resists in industry standard 0.26 N tetramethylammonium hydroxide (TMAH) solution. The well resolved negative tone micro features of homopoly(TPMA) and 2.0%-poly(FEMA-*co*-TPMA) resists are shown in Fig. 4. Based on the micro-patterning ability of poly(TPMA) and 2.0%-poly(FEMA-*co*-TPMA) resists under DUVL conditions, we tested the nano-patterning potentials of these resists under

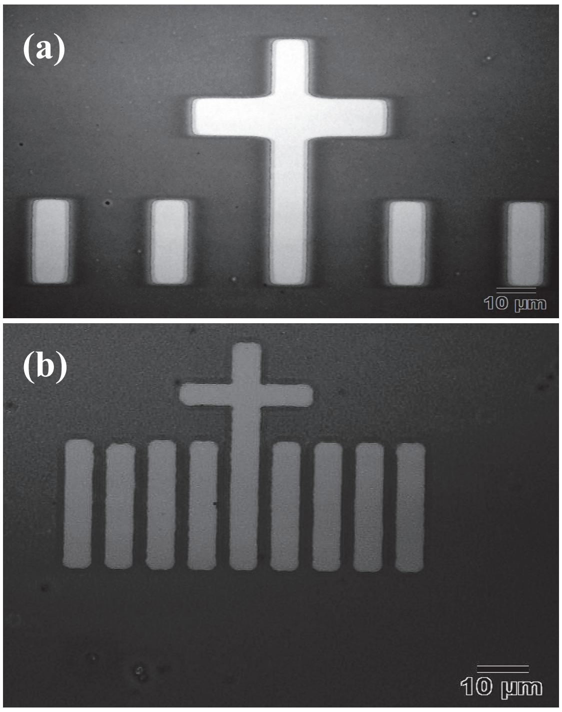

Fig. 4. Micron sized features patterned using DUV-254 nm tool: (a) 10 µm features of homo poly-(TPMA) resist; (b) 5 µm features of hybrid 2.0%-poly-(FEMA-*co*-TPMA) copolymer resist.

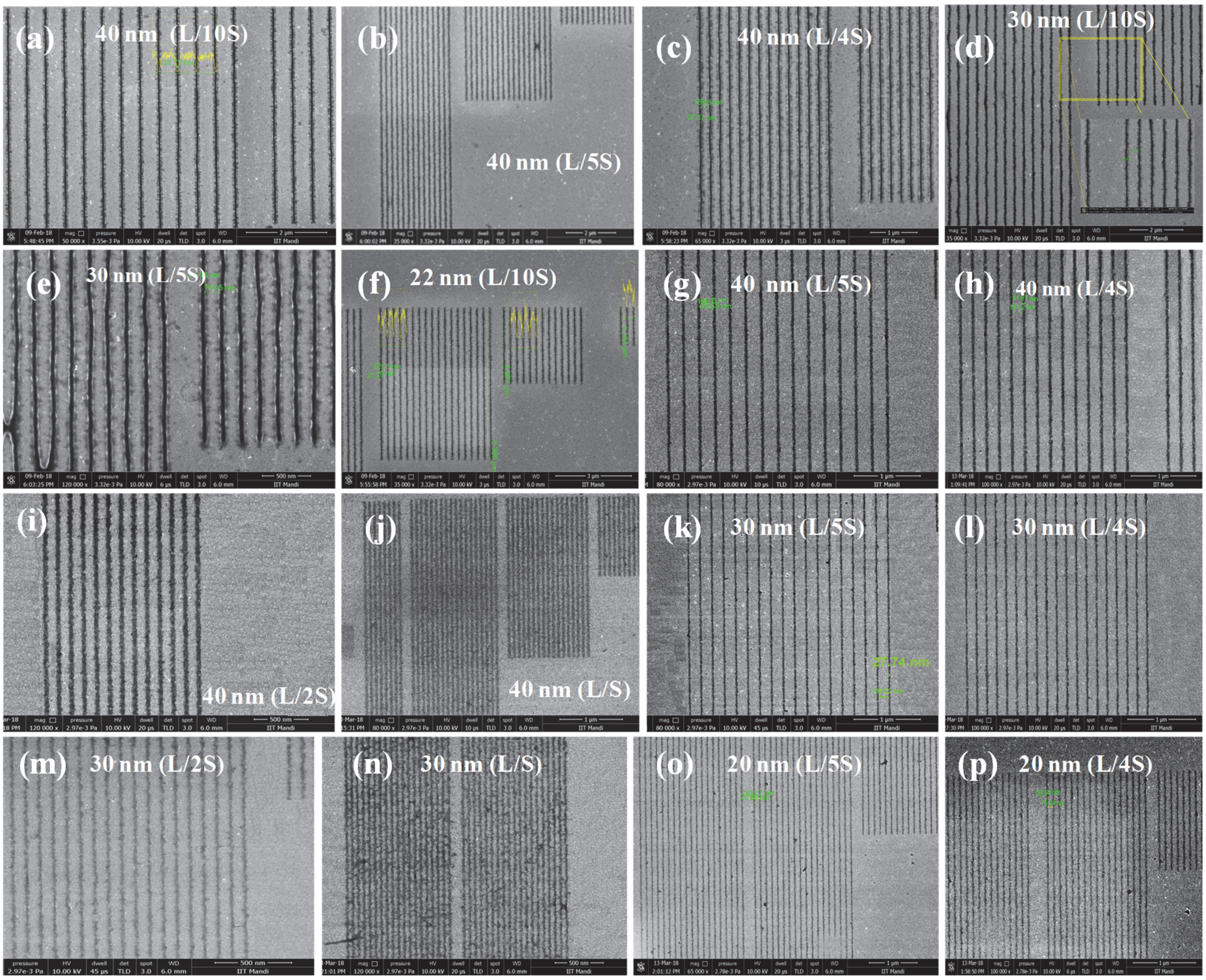

Fig. 5. SEM images of the nano line features with different line/space (L/10S-L/S) characteristics patterned under EBL: (a-c) 40 (L/10S-L/4S); (d-e) 30 (L/10S & L/5S) and (f) 22 nm (L/10S) line patterns of poly(TPMA) at the dose 950 μC/cm^2; (g-j) 40 nm (L/5S-L/S), (k-n) 30 nm, (L/5S-L/S) and (o-p) 20 nm (L/5S-L/4S) features of 2.0%-poly(FEMA-*co*-TPMA) resist at the dose 500 μC/cm^2.

e-beam lithography tool. The experimental parameters employed in micro- patterning studies for spin coating, pre-bake, post-bake, development etc. were applied in nano patterning studies as well. Various exposure doses starting from 100 to 1000 μC/cm^2 were tested to find out the optimum exposure dose parameters (i.e. the dose required to pattern collapse free nano-features on silicon substrate). The calculated optimum dosages for poly(TPMA) and 2.0%-poly(FEMA-*co*-TPMA) resists were 950 and 500 μC/cm^2, respectively. The application of e-beam doses of 100-500 μC/cm^2 on poly(TPMA) films revealed insufficient dose characteristics and yielded no patterns at the nano level. However, on increasing the exposure dose values from 600 to 1000 μC/cm^2, the resist films patterned nano-features. For example, the well resolved collapse-free 40 nm (L/10S to L/4S (line/space)) line patterns obtained from the poly(TPMA) at the e-beam dose 950 μC/cm^2 are given in Figs. 5(a-c). Similarly, the 30 nm (L/10S & L/5S) and 22 nm (L/10S) line patterns exhibited by the resist are given in Figs. 5(d-f). However, the efforts to achieve collapse free line patterns using poly(TPMA) at the critical dimensions of 40 nm (L/3S-L/S), 30 nm (L/4S-L/S), and 22 nm (L/5S-L/S) were unsuccessful due to the line buckling observed at such resolutions. For example, the buckled 30 nm (L/4S) features exhibited by poly(TPMA) at the e-beam dose 950 μC/cm^2 is given in Fig. 6. On the other hand, the hybrid 2.0%-poly(FEMA-*co*-TPMA) resist exhibited 40 nm and 30 nm line patterning with different line/space features (L/5S-L/S) at the e-beam dose of 500 μC/cm^2, indicating enhanced sensitivity and resolution as compared to that of the poly(TPMA) resist, Figs. 5(g-n). Unlike poly(TPMA) resist, the hybrid 2.0%-poly(FEMA-*co*-TPMA) resist patterned high resolution 20 nm (L/5S and L/4S) line patterns as shown in Figs. 5(o&p). The enhanced sensitivity and resolution exhibited by 2.0%-poly(FEMA-*co*-TPMA) resist may be attributed to the effect of the OMC unit present in it.

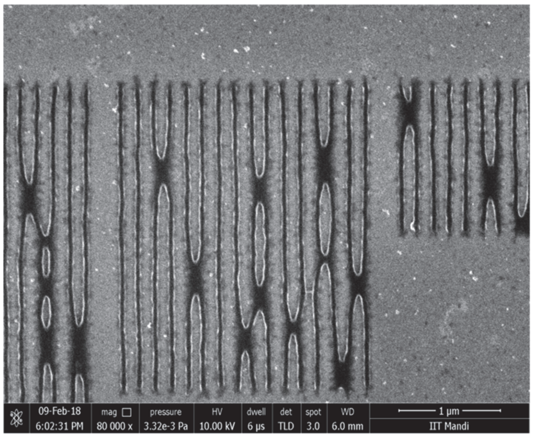

Fig. 6. SEM image of 30 nm line patterns with L/4S (line/space) features exhibited by the resist poly(TPMA) at the dose 950 μC/cm^2.

Further, in order to estimate the sensitivity of the resists, the patterned thinfilms were subjected to normalized remaining thickness (NRT) curve analysis [16] by plotting the residual film thickness *vs* the e-beam exposure dose values (Fig. 7(a&b)). Various e-beam exposure doses starting from 30-770 μC/cm^2 were considered for sensitivity curve analysis. It was noted that the residual thickness of the poly(TPMA) and 2.0%-poly(FEMA-*co*-TPMA) resists increases gradually with increase in the exposure dose values, indicating negative tone nature of these resists (Fig. 7(a&b)). The sensitivity and contrast (γ) of poly(TPMA) were calculated from the contrast curve analysis as 270 μC/cm^2 and 5.23 respectively (Fig. 7(a)). Similarly, the observed sensitivity and *γ* values for 2.0%-poly(FEMA-*co*-TPMA) resist were 153 μC/cm^2 and 1.98, respectively (Fig. 7(b)). These studies clearly indicate that there is an improvement in the sensitivity of the copolymer resist as compared to that of the homo polymer resist. As noticed above, the enhanced sensitivity of the hybrid polymer could be due to the attached ferrocene units in its polymer backbone. The resists reported in this study are directly sensitive to the radiations and hence belong to the class of non-chemically amplified (n-CAR) resists.

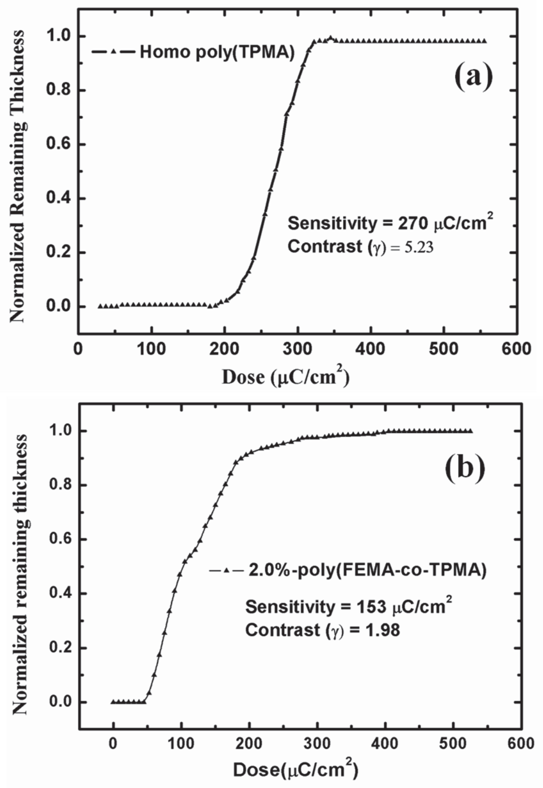

Fig. 7. Normalized remaining thickness *vs* e-beam dose characteristics (a) poly(TPMA) and (b) 2.0%-poly(FEMA-*co*-TPMA) resist.

Aryl sulfonates such as imino/imido sulfonates and other related compounds are well explored for their photochemical behaviours [43,44]. In such compounds, the sensitive N–O bond undergoes photo cleavage and releases the radical sulfonate ($RSO_3^\cdot$) moiety upon irradiation, which further reacts with the medium and generates strong triflic acid products [43,44]. Therefore, imino/imido sulfonate derivatives are utilized as photo acid generators (PAGs) for CARs structural transformations [44]. M. Fagnoni *et al.* reported a series of aryl tosylates based non-ionic PAGs and their photochemical characteristics were evaluated under DUV-254 nm radiation [43]. These studies revealed the formation of phenol derivatives, photo-Fries adducts as well as *p*-toluenesulfinic/sulfonic acid derivatives from the aryl tosylates upon irradiation [43]. In the present study, the poly(TPMA) and 2.0%-poly(FEMA-*co*-TPMA) resist structures are made up of radiation sensitive aryl tosylates. Therefore, we assume a similar structural decomposition mechanism as reported earlier for aryl tosylates upon interaction of the resist films with high energy radiations. Polarity switching results accompanying changes in the resist structure from hydrophobic poly-tosylates to hydrophilic poly-phenol derivatives. These emergent structural transformations lead to the negative tone patterning upon developing the exposed thin films with 1,4-dioxane, which dissolves only the unexposed portions while leaving behind the exposed portions undissolved. Therefore, the present resist formulations act as negative tone resists with 1,4-dioxane developer.

4. Conclusion

Starting from non-ionic aryl tosylate and organometallic ferrocene monomers, we have developed a new class of homo and hybrid polymer resists, poly(TPMA) and 2.0%-&4.0%-poly(FEMA-*co*-TPMA), for micro/nano lithography applications. Poly(TPMA) and 2.0%-poly(FEMA-*co*-TPMA) resists exhibited micro patterning properties under DUVL patterning tool as negative tone resists with 1,4-dioxane developer. In addition, these polymers acted as photo-resists under e-beam lithography tool for patterning nano-line features. The poly(TPMA) showed 40 nm (L/10S to L/4S), 30 nm (L/10S & L/5S) and 22 nm (L/10S) line patterns at the e-beam dose of 950 $\mu C/cm^2$, whereas, the hybrid 2.0%-poly(FEMA-*co*-TPMA) resist exhibited 40 nm (L/5S to L/S), 30 nm (L/5S to L/S), and 20 nm (L/5S & L/4S) line patterns at the e-beam dose 500 $\mu C/cm^2$. The sensitivity and contrast (γ) of the homo poly(TPMA) and hybrid 2.0%-poly(FEMA-*co*-TPMA) polymer resists were calculated from the NRT curve analysis as 270 $\mu C/cm^2$; 5.2 and 153 $\mu C/cm^2$; 1.98 respectively. These results, therefore, conclude that the inclusion of a small amount of ferrocene units in 2.0%-poly(FEMA-*co*-TPMA) resist resulted in it exhibiting enhanced sensitivity and resolution as compared to poly(TPMA) resist.

Acknowledgements

Authors thank the Department of Science and Technology (DST) and Technology Systems Development Program (TSDP), India for the financial support. Sanctioned project reference number: DST/TSG/AMT/2015/634. The Authors acknowledge the use of the CEN, EBL facility at IIT Bombay. P. G. Reddy thanks the Council of Scientific and Industrial Research (CSIR), New Delhi, India for a senior research fellowship. M. G. Moinuddin thanks the Ministry of Electronics & Information Technology for a junior research fellowship under the Visvesvaraya Ph.D Scheme.

References

1. G. Moore, *Electronics,* **38** (1965) 114.
2. H. P. Alesso and C. F. Smith, "*Connections: patterns of discovery*", John Wiley & Sons, New Jersey, (2008).
3. K. L. Berkowski, K. N. Plunkett, Q. Yu, and J. S. Moore, *J. Chem. Educ.,* **82** (2005) 1365.
4. Y. Xia and G. M. Whitesides, *Annu. Rev. Mater. Sci.,* **28** (1998) 153.
5. S. Ghosh, C. P. Pradeep, S. K. Sharma, P. G. Reddy, S. P. Pal, and K. E. Gonsalves, *RSC Adv.,* **6** (2016) 74462.
6. L. Li, X. Liu, S. Pal, S. Wang, C. K. Ober, and E. P. Giannelis, *Chem. Soc. Rev.,* **46** (2017) 4855.
7. ITRS, "The International Technology Roadmap for Semiconductors-2015", available via the Internet at https://www.semiconductors.org/clientuploads/Research_Technology/ITRS/2015/0_2015%20ITRS%202.0%20Executive%20Report%20(1).pdf.
8. M. Neisser and S. Wurm, *Adv. Opt. Technol.,* **4** (2015) 235.
9. H. Ito, *Adv. Polym. Sci.,* **172** (2005) 37.
10. S. A. M. Donald, C. G. Willson, and J. M. J. Frechet, *Acc. Chem. Res.,* **27** (1994) 151.
11. M. D. Stewart, K. Patterson, M. H. Somervell, and C. G. Willson, *J. Phys. Org. Chem.,* **13** (2000) 767.
12. E. Reichmanis and L. F. Thompson, *Chem. Rev.,* **89** (1989) 1273.
13. J. W. J. Thackeray, *J. Micro/Nanolith., MEMS, MOEMS,* **10** (2011) 033009.
14. P. P. Naulleau, C. N. Anderson, L. M. Baclea-an, P. Denham, S. George, K. A. Goldberg, G. Jones, B. Mc Clinton, R. Miyakawa, S. Rekawa, and N. Smith, *Proc. SPIE,* **7972** (2011) 797202.
15. Y. Wei, M. Bender, W. D. Domke, A. Laessig, M. Sebald, S. Trogisch, and D. Back, *Proc. SPIE,* **6519** (2007) 65190R.
16. P. G. Reddy, S. P. Pal, P. Kumar, C. P. Pradeep, S. Ghosh, S. K. Sharma, and K. E. Gonsalves, *ACS Appl. Mater. Interfaces,* **9** (2017) 17.

17. K. J. Lawrie, I. Blakey, J. P. Blinco, H. H. Cheng, R. Gronheid, K. S. Jack, I. Pollentier, M. J. Leeson, T. R. Youkin, and A. K. Whittaker, *J. Mater. Chem.,* **21** (2011) 5629.
18. A. Yu, H. Liu, J. P. Blinco, K. S. Jack, M. Leeson, T. R. Younkin, A. K. Whittaker, and I. Blakey, *Macromol. Rapid Commun.,* **31** (2010) 1449.
19. M. Wang, N. D. Jarnagin, C. T. Lee, C. L. Henderson, W. Yueh, J. M. Roberts, and K. E. Gonsalves, *J. Mater. Chem.,* **16** (2006) 3701.
20. K. E. Gonsalves, M. Wang, C. T. Lee, W. Yueh, M. T. Tapia, N. Batinad, and C. L. Henderson, *J. Mater. Chem.,* **19** (2009) 2797.
21. O. Yildirim, E. Buitrago, R. Hoefnagels, M. Meeuwissen, S. Wuister, G. Rispens, A. V. Oosten, P. Derksa, J. Finders, M. Vockenhuber, and Y. Ekinci, *Proc. SPIE,* **10143** (2017) 101430Q.
22. D. D. Simone, Y. Vesters, A. Shehzad, G. Vandenberghe, P. Foubert, C. Beral, D. V. D. Heuvel, M. Mao, and F. Lazzarino, *Proc. SPIE,* **10143** (2017) 101430R.
23. N. Mojarad, M. Hojeij, L. Wang, J. Gobrecht, and Y. Ekinci, *Nanoscale,* **7** (2015) 4031.
24. P. G. Reddy, N. Mamidi, P. Kumar, S. K. Sharma, S. Ghosh, K. E. Gonsalves, and C. P. Pradeep, *RSC Adv.,* **6** (2016) 67143.
25. H. W. Ro, V. Popova, L. Chen, A. M. Forster, Y. F. Ding, K. J. Alvine, D. J. Krug, R. M. Laine, and C. L. Soles, *Adv. Mater.,* **23** (2011) 414.
26. B. Cardineau, R. D. Re, M. Marnell, H. A. Mashat, M. Vockenhuber, Y. Ekinci, C. Sarma, D. A. Freedman, and R. L. Brainard, *Microelectron. Eng.,* **127** (2014) 44.
27. V. Kalyani, V. S. V. Satyanarayana, V. Singh, C. P. Pradeep, S. Ghosh, S. K. Sharma, and K. E. Gonsalves, *Chem. Eur. J.,* **21** (2015) 2250.
28. P. G. Reddy, P. Kumar, S. Ghosh, C. P. Pradeep, S. K. Sharma, and K. E. Gonsalves, *Mater. Chem. Front.,* **1** (2017) 2613.
29. M. Sortland, J. Hotalen, R. D. Re, J. Passarelli, M. Murphy, T. S. Kulmala, Y. Ekinci, M. Neisser, D. A. Freedman, and R. L. Brainard, *J. Micro/Nanolith., MEMS, MOEMS,* **14** (2015) 043511.
30. J. Hotalen, M. Murphy, W. Earley, M. Vockenhuber, Y. Ekinci, D. A. Freedman, and R. L. Brainard, *Proc. SPIE,* **10143** (2017) 1014309.
31. J. Passarelli, M. Murphy, R. D. Re, M. Sortland, L. Dousharm, M. Vockenhuber, Y. Ekinci, M. Neisser, D. A. Freedman, and R. L. Brainard, *Proc. SPIE,* **9425** (2015) 94250T.
32. K. Kasahara, H. Xu, V. Kosma, J. Odent, E. P. Giannelis, and C. K. Ober, *Proc. SPIE,* **10143** (2017) 1014308.
33. M. Trikeriotis, M. Krysak, Y. S. Chung, C. Ouyang, B. Cardineau, R. Brainard, C. K. Ober, E. P. Giannelis, and K. Cho, *J. Photopolym. Sci. Technol.,* **25** (2012) 583.
34. R. Pietschnig, *Chem. Soc. Rev.,* **45** (2016) 5216.
35. R. Tong, Y. Zhao, L. Wang, H. Yu, F. Ren, M. Saleem, and W. A. Amer, *J. Organomet. Chem.,* **755** (2014) 16.
36. C. Engtrakul and L. R. Sita, *Nano Lett.,* **1** (2001) 541.
37. R. Liu, S. H. Ke, H. U. Branger, and W. Yang, *Nano Lett.,* **5** (2005) 1959.
38. Y. Matsuura and K. Matsukawa, *Chem. Phys. Lett.,* **436** (2007) 224.
39. J. Zhang, K. Cao, X. S. Wang, and B. Cui, *Chem. Commun.,* **51** (2015) 17592.
40. V. S. V. Satyanarayana, V. Singh, V. Kalyani, C. P. Pradeep, S. Sharma, S. Ghosh, and K. E. Gonsalves, *RSC Adv.,* **4** (2014) 59817.
41. B. S. B. Clendenning, S. Aouba, M. S. Rayat, D. Grozea, J. B. Sorge, P. M. Brodersen, R. N. S. Sodhi, Z. H. Lu, C. M. Yip, M. R. Freeman, H. E. Ruda, and I. Manners, *Adv. Mater.,* **16** (2004) 215.
42. W. Y. Chan, S. B. Clendenning, A. Berenbaum, A. J. Lough, S. Aouba, H. E. Ruda, and I. Manners, *J. Am. Chem. Soc.,* **127** (2005) 1765.
43. E. Torti, G. D. Giustina, S. Protti, D. Merli, G. Brusatin, and M. Fagnoni, *RSC Adv.,* **5** (2015) 33239 and references cited therein.
44. R. A. Lawson, D. E. Noga, L. M. Tolbert, and C. L. Henderson, *J. Micro/Nanolith. MEMS MOEMS,* **8** (2009) 043010.
45. W. Xu, T. Li, G. Li, Y. Wu, and T. Miyashita, *J. Photochem. Photobiol. A: Chem.,* **219** (2011) 50.